

Mesoscopic resistor as a self-calibrating quantum noise source

N. Bergeal,^{1,2} F. Schackert,² L. Frunzio,² D. E. Prober,² and M. H. Devoret²

¹Laboratoire de Physique et d'Etude des Matériaux – UMR8213-CNRS, ESPCI ParisTech, UPMC, 10 Rue Vauquelin, 75005 Paris, France

²Departments of Physics and Applied Physics, Yale University, New Haven, Connecticut 06520-8284, USA

(Received 24 February 2012; accepted 26 April 2012; published online 15 May 2012)

We present a method for the measurement of the noise of microwave amplifiers operating at the single photon level. It is based on the shot noise produced by a nanowire resistor in the hot electron regime. This noise source is simply controlled by a dc current and offers the advantage of being self-calibrating. After testing the noise source with a cryogenic high electron mobility transistor amplifier, we demonstrate its usefulness by calibrating a Josephson parametric amplifier operating near the quantum limit. © 2012 American Institute of Physics. [<http://dx.doi.org/10.1063/1.4717462>]

Ultra low noise amplifiers working in the microwave frequency range are essential for measuring the extremely small signal involved in quantum information processing devices such as superconducting qubits.^{1–4} Theoretically, the minimum noise added by an amplifier to the signal it processes is imposed by quantum mechanics.⁵ For a phase-preserving amplifier in the large gain limit, this minimum noise amounts to half a photon at the signal frequency referred to the input ($\frac{1}{2}\hbar\omega$). Following the pioneering work of Yurke,⁶ several groups have recently developed amplifiers that approach the quantum limit, using Josephson parametric amplifier concepts^{7–10} or dc superconducting quantum interference devices.¹¹ In all cases, assessing the noise characteristics of an amplifier requires the use of a well calibrated source capable of producing a noise with tunable intensity of order one photon. In this article, we report the operation of such noise source based on a nanowire resistor of mesoscopic length, which offers the advantage of self-calibration.

In the standard noise calibration method (Y factor measurement), the output noise power N^{out} of the amplifier is measured for two different temperatures T_1 and T_2 of a matched load connected to its input. The noise added by the amplifier N^{added} is then given by $[N^{\text{out}}(T_1)T_2 - N^{\text{out}}(T_2)T_1]/(T_2 - T_1)$. Although this method is efficient for calibrating the noise of a cryogenic amplifier operating at 4.2 K for instance, it is not adapted to the calibration of an amplifier operating near the quantum limit in a dilution refrigerator. The problem is to control precisely the temperature of the load. One possible way to realize the calibration is to use a mechanical switch to connect alternatively the input of the amplifier to two loads located at different temperature stages of the fridge.^{6,7} However, at low temperature, the thermal anchoring of the load and the determination of the switch attenuation are not easy. In addition, the speed of a mechanical switch is also limited. Ideally, a microwave component whose noise would be a universal known function of an external controllable parameter would solve the problem. The shot noise of a normal-insulator-normal tunnel junction approaches this requirement.¹² However, the junction capacitance filters the noise at microwave frequency in a manner which cannot be easily determined. Furthermore since suitable tunnel junctions have so far only been reliably fabricated

with Al films, the superconductivity of Al needs to be entirely suppressed by a small permanent magnet. In this paper, we explore an alternative device based on a metallic nanowire which avoids the two problems mentioned above.

A metallic wire resistor exhibits several regimes of shot noise depending on its length L relative to the characteristic length scales involved in the electron motion.¹³ In a typical metal, these length scales are from the shortest to the longest: the elastic mean free path l , the phase breaking length L_ϕ , the inelastic electron scattering length L_{e-e} , and the electron-phonon interaction length L_{e-ph} . In this article, we focus on the hot electron regime where $L_{e-e} \ll L \ll L_{e-ph}$. We assume that the resistor wire is embedded between two ideal thermal reservoirs in which a constant electron temperature T_0 is imposed. In this case, when a dc voltage is applied across the wire, the electrons accelerating during their travel through the resistor thermalize their kinetic energy via electron-electron interactions.¹³ In steady state, the cooling of the nanowire occurs only by diffusion of hot electrons to the cold reservoirs, a process obeying the Wiedemann-Franz law. As a result, the equilibrium electron temperature profile over the length of the microbridge (Fig. 1(d))¹⁴ is

$$T_e(x) = T_0 \sqrt{1 + \frac{x}{L} \left(1 - \frac{x}{L}\right) \frac{3e^2 V^2}{\pi^2 k_B^2 T_0^2}}, \quad (1)$$

where V is the dc voltage across the resistor and T_0 is the temperature of the reservoirs.

The effective temperature controlling the noise of the nanowire is defined by integrating over the length of the nanowire,

$$T^{\text{eff}} = \frac{1}{L} \int_0^L T_e(x) dx = \frac{T_0}{2} \left[1 + \left(v + \frac{1}{v} \right) \arctan(v) \right], \quad (2)$$

where $v = \frac{\sqrt{3}}{2\pi} \frac{eV}{k_B T_0}$. Note that we have assumed here that the resistance of the nanowire is independent of temperature in the range of interest.

The noise power spectral density (PSD) resulting from this hot electron temperature is given by

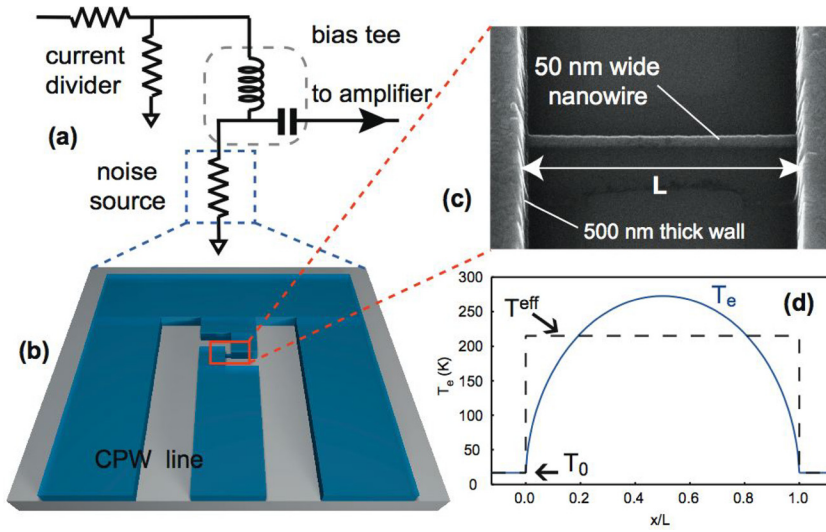


FIG. 1. (a) Hot electron nanowire noise source in its embedding measurement circuit. (b) Schematic of the connection of the nanowire in a thick $50\ \Omega$ coplanar waveguide transmission line. (c) SEM picture of the nanowire. (d) Temperature profile $T_e(x)$ (solid line) along the nanowire and effective temperature T_e^{eff} (dashed line) for a bias voltage $V = 85\ \mu\text{V}$. At $x=0$ and $x=L$, the temperature of the reservoirs is set by the temperature of the fridge T_0 (17 mK in this example).

$$S^{\text{HE}}(\omega) = \frac{\hbar\omega}{2} \coth\left(\frac{\hbar\omega}{2k_B T^{\text{eff}}(V)}\right), \quad (3)$$

where the effective electronic temperature of the resistor T^{eff} is given by the expression (2). Here, the dimension of $S^{\text{HE}}(\omega)$ is Watt per Hertz. For $k_B T^{\text{eff}} \gg \hbar\omega$, this expression reduces to the classical Johnson noise.¹⁵ This noise source has several advantages: (i) it is simply controlled by a dc voltage (or current), (ii) it responds at the microsecond scale,¹⁶ (iii) the heating of the reservoirs is negligible compared to typical cooling powers at low temperature, (iv) it is self-calibrating (or, in other words, absolute) since there is no unknown parameter in the expression of the noise PSD (Eq. (3)) as long as the voltage can be reliably determined. Note that for $l \ll L \ll L_{e-e}$, the electrons diffuse without interaction but their population statistic is no longer described by a Fermi distribution. In this quantum shot noise (QSN) regime and for a large number of channels, the predicted noise power spectral density is¹⁷

$$S^{\text{QSN}}(\omega) = \frac{1}{3} \left[(eV + \hbar\omega) \coth\left(\frac{eV + \hbar\omega}{2k_B T}\right) + (eV - \hbar\omega) \coth\left(\frac{eV - \hbar\omega}{2k_B T}\right) + 4\hbar\omega \coth\left(\frac{\hbar\omega}{2k_B T}\right) \right]. \quad (4)$$

Although this regime is in principle suitable to realize a noise source, it is in practice more difficult to implement than the hot electron regime due to the short length of the wire.

Using e-beam lithography and a double angle evaporation technique, we have fabricated nominally $50\ \Omega$ (at the operating temperature) copper nanowires with length $3\ \mu\text{m}$ to $4\ \mu\text{m}$, width of $50\ \text{nm}$ and thickness $20\ \text{nm}$ to $28\ \text{nm}$. They were embedded in a $500\ \text{nm}$ thick $50\ \Omega$ coplanar waveguide transmission line which played the role of ideal thermal reservoirs (Fig. 1). We first characterized the samples using a $38\ \text{dB}$ gain cryogenic high electron mobility transistor (HEMT) amplifier operating in the frequency band $1\text{--}2\ \text{GHz}$ with a noise temperature of approximately $5\ \text{K}$. The samples

were mounted on a sample holder using a RF coaxial connector and were anchored to the last temperature stage of a ^3He cryostat of temperature T_0 . The sample chip was connected to the direct port of a bias-Tee. A dc current is applied to the noise source using a cold current divider so that only a small part I of the total current is sent to the dc port of the bias-Tee. Finally, the high frequency port of the bias-Tee is connected via three isolators (Pamtech $1.2\text{--}1.8\ \text{GHz}$) to the input port of the HEMT amplifier placed at $4.2\ \text{K}$, before further amplification at room temperature. Using a commercial diode (band $1\text{--}2\ \text{GHz}$), we measured the noise PSD at the output of the amplification chain as a function of the voltage V across the nanowire for two different temperatures $T_0 = 260\ \text{mK}$ and $T_0 = 1685\ \text{mK}$ of the cryostat (Fig. 2).

The experimental noise PSD, referred to the output of the noise source can be compared to the theoretical expected output noise PSD

$$S^{\text{th}} = G_t(S^{\text{HE}} + S^{\text{add}}), \quad (5)$$

where G_t is a free parameter corresponding the total gain and attenuation of the measurement chains, S^{HE} is the noise produced by the noise source given by Eq. (3), and S^{add} is the effective noise added by the HEMT amplifier. The latter has

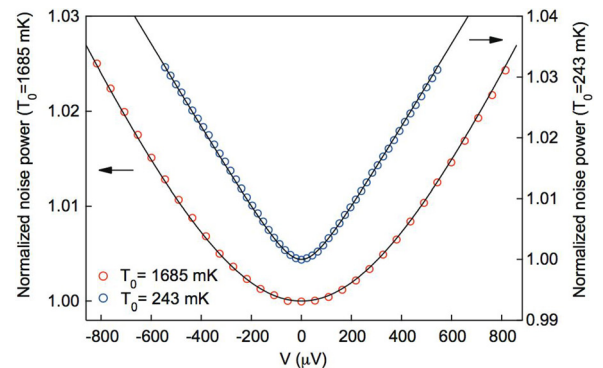


FIG. 2. Noise of the hot electron source normalized by the value at $V=0\ \mu\text{V}$, measured at the output of the refrigerator and integrated over the band $1\text{--}2\ \text{GHz}$ as a function of the dc voltage across the nanowire, at two different temperatures T_0 . The open symbols correspond to the experimental data and the solid lines to the theoretical expression (5).

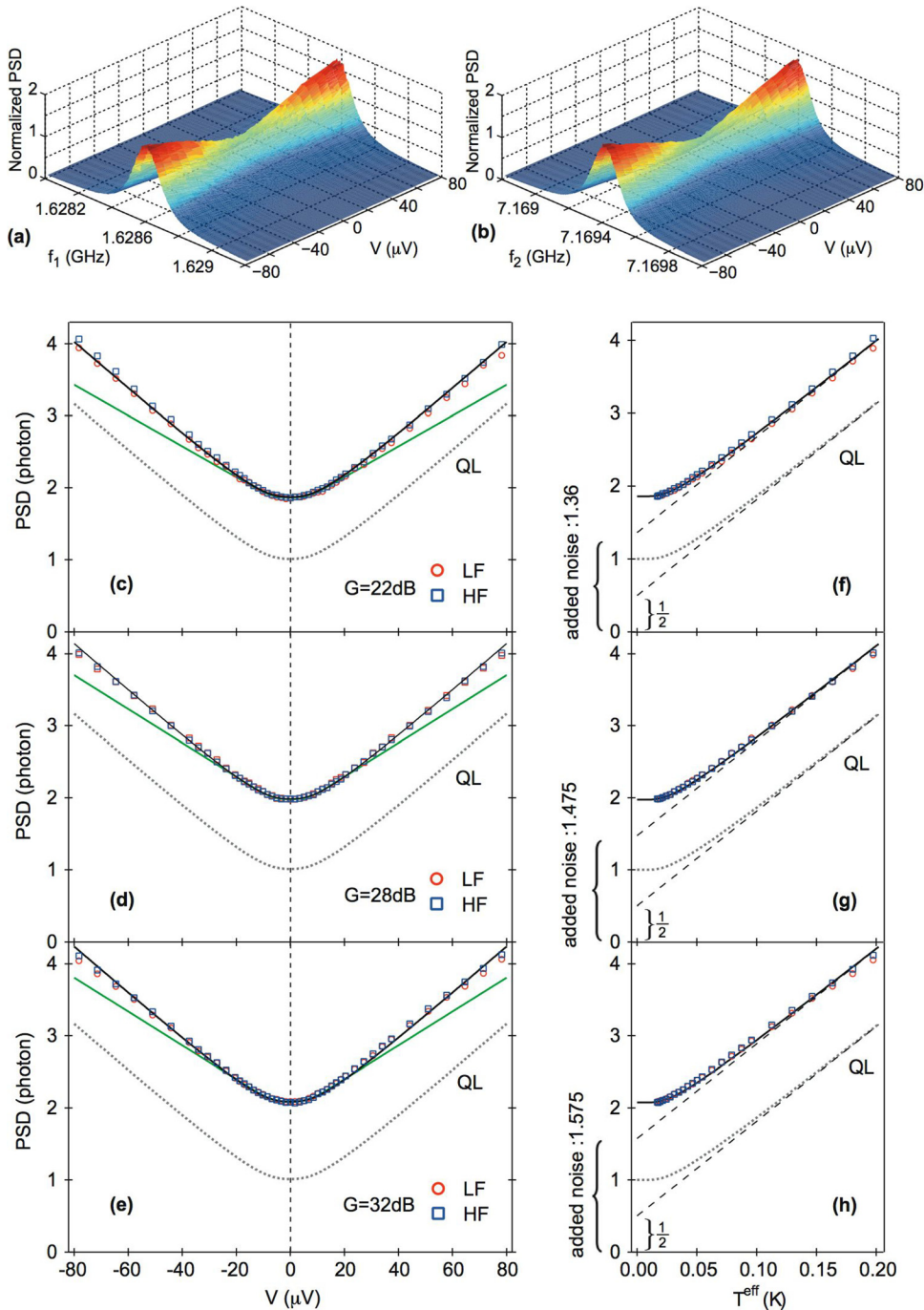


FIG. 3. (a) and (b) Normalized noise PSD at the output of the refrigerator on the LF port (a) and HF port (b) as a function of noise frequency $f_{1(2)}$ and voltage V across the resistor measured for a 32 dB gain. (c)–(e) Noise PSD referred to the output of the noise source, integrated over a 1 MHz frequency band and expressed in photon units, as a function of V for three different gains. The experimental data (open symbols) are fitted by the theoretical expression (5) of the hot-electron regime (black full lines). The best fits give an added noise of 1.36, 1.475, and 1.575 photon (increasing gain). The theoretical quantum limit (QL) is indicated as reference (dotted lines). The green line corresponds to the expression of quantum shot noise (Eq. (4)). (f)–(h) Noise PSD at the LF and HF port plotted as a function of effective temperature. Open symbols correspond to experimental data and full lines to theory. The theoretical QL is indicated as reference (dotted lines). The dashed lines indicate high temperature variation.

to be understood taking into account the microwave set-up (bias-Tee, isolators, attenuators and coaxial cables) between the noise source and the amplifier. We obtain a good agreement between the theoretical and experimental variations of noise versus voltage indicating that the noise source is well in the hot electron regime. We have verified that computing the shot noise of the resistor using Eq. (3) yields the same result, at the percentage precision level, as when the full space-dependent spectral density of noise is taken into account. The best fits give the system noise temperature $T_N^{\text{sys}1} = \frac{S^{\text{add}}}{k_B} \simeq 36$ K for $T_0 = 243$ mK and $T_N^{\text{sys}1} \simeq 39$ K for $T_0 = 1.685$ K. The small imprecision in the value of T_N can be explained by the fact that the range of source temperature explored in the noise measurement ($V = 870 \mu\text{V}$ corresponds to $T^{\text{eff}} = 2.2$ K according to expression (2)) is much smaller

than $T_N^{\text{sys}1}$. Although this experiment shows that it is possible to measure noise temperatures of several tens of Kelvin with a rather good precision, the real interest of this mesoscopic noise source lies in its ability of measuring precisely ultra-low noise temperatures in the vicinity of the quantum regime $k_B T_N \simeq \hbar\omega$. We now address more refined characterisation of the noise of the nanowire in this regime, using a superconducting parametric amplifier, nicknamed Josephson parametric converter (JPC) recently developed in our group (Refs. 9, 18, and 19).

Limiting the description to the low-amplitude signals processed by the amplifier, the device has two ports: a low frequency (LF) port driven at carrier frequency f_1 and a high frequency (HF) port, driven at carrier frequency f_2 . When the pump frequency is set as the sum $f_1 + f_2$, the JPC operates as

a phase-preserving amplifier in reflection and as a phase conjugating frequency converter with gain in transmission.¹⁸ Each port of the JPC is connected to a circulator in order to separate the outgoing signal from the incoming one. The noise source and the JPC were anchored at the last stage of a dilution refrigerator with a base temperature $T_0 = 17$ mK. In this second experimental set-up, the noise source is connected to the low frequency port of the JPC through a bias-Tee and a circulator. The HF port is connected to a 50 Ω load through the circulator of this port. The noise coming out of both ports of the JPC (LF and HF) is further amplified at the 4.2 K stage by cryogenic HEMT amplifiers. Isolators and circulators placed at 17 mK, 60 mK, and 800 mK stages minimize the backaction of the HEMT amplifiers on the JPC. As the bandwidth of the JPC is much narrower than the typical bandwidth of commercial diodes, the noise on each port was directly recorded with a spectrum analyser.

Figures 3(a) and 3(b) display the output noise PSD as a function of the voltage V across the nanowire, measured at both ports for a JPC gain of 32 dB. In Figure 3(c), we show the noise integrated over a 1 MHz band around the center frequencies (1.6286 GHz for the LF port and 7.1694 GHz for the HF port) of the amplification bandwidth as a function of the voltage V for three different values of gain. The noise expressed in photon number refers to the output of the noise source, which is equivalent to the input of the JPC, assuming a negligible attenuation between the two elements. The good agreement between theory and experimental data confirms that the resistor is well in the hot electron regime in this temperature range, in agreement with previous studies.²⁰ In particular, it is not possible to fit the data using the expression for the quantum shot noise regime $l \ll L \ll L_{e-e}$ (Eq. (4)) (Fig. 3 green lines). Having verified that the noise source behaves as expected, we now demonstrate its usefulness in assessing the added noise of the JPC (see panels c, d, and e in Fig. 3). For a 22 dB gain, we obtain an added noise of 1.36 photon, corresponding to $S^{\text{add}} = 2.72 \times S^{\text{QL}}$, where $S^{\text{QL}} = \frac{1}{2}hf_1$ is the noise added by a perfect quantum limited amplifier. Note that the amount of added noise measured at the LF and HF ports are identical although they are centered around different frequencies. In the same figure, for comparison, we plot the theoretical result corresponding to the ideal case of both perfect nanowire and quantum limited amplifier. The noise is found to increase slightly with the gain: 1.475 photon and 1.575 photon for 28 dB (d) and 32 dB gains (e), which could be due to the imperfect isolation of circulators. In Figure 3, panels f, g, and h, the voltage axis has been converted into a temperature scale using the expression (2). The noise added by the amplifier is the vertical intercept of the dashed lines corresponding to the asymptotic variation of noise with temperature. Converting the upper bound on the added noise S^{add} into the system noise temperature, we found $T_N^{\text{sys}2} = 110$ mK for the 22 dB gain, which shows that the JPC is 20 to 40 times better than the best commercial HEMT amplifiers.

In conclusion, we have developed a method to characterize ultra low-noise amplifiers using the hot electron shot noise regime of a metallic nanowire. The device operation is based on the relation between the voltage across a nanowire and the RF noise it produces, much like in the tunnel junction shot noise thermometry,¹² which has the advantages of self-calibration, dc control, and fast response. In addition, our nanowire is easy to fabricate and has simpler RF characteristics. To illustrate the method, we have measured the noise of a parametric amplifier, which operates in the vicinity of the quantum limit.

We acknowledge useful discussions with D. F. Santa-vecchia, B. Huard, N. Roch, S. M. Girvin, and R. J. Schoelkopf. This research was supported by the US National Security Agency through the US Army Research Office grant W911NF-05-01-0365, the W. M. Keck Foundation, the US National Science Foundation through Grant Nos. DMR-0653377 and DMR-0907082. L.F. acknowledges partial support from CNR-Istituto di Cibernetica. M.H.D. also acknowledges partial support from the College de France and from the French Agence Nationale de la Recherche.

- ¹A. Wallraff, D. I. Schuster, A. Blais, L. Frunzio, R.-S. Huang, J. Majer, S. Kumar, S. M. Girvin, and R. J. Schoelkopf, *Nature* **431**, 162–167 (2004).
- ²A. Lupaşcu, S. Saito, T. Picot, P. C. De Groot, C. J. P. M. Harmans, and J. E. Mooij, *Nat. Phys.* **3**, 119–123 (2007).
- ³M. A. Sillanpää, J. I. Park, and R. W. Simmonds, *Nature* **449**, 438–442 (2007).
- ⁴J. Majer, J. M. Chow, J. M. Gambetta, J. Koch, B. R. Johnson, J. A. Schrier, L. Frunzio, D. I. Schuster, A. A. Houck, A. Wallraff *et al.*, *Nature* **449**, 443–447 (2007).
- ⁵C. M. Caves, *Phys. Rev. D* **26**, 1817–1839 (1982).
- ⁶B. Yurke, L. R. Corruccini, P. G. Kaminsky, L. W. Rupp, A. D. Smith, A. H. Silver, and R. W. Simon, *Phys. Rev. A* **39**, 2519–2533 (1989).
- ⁷M. A. Castellanos-Beltrana, K. D. Irwin, G. C. Hilton, L. R. Vale, and K. W. Lehnert, *Nat. Phys.* **4**, 929–931 (2008).
- ⁸T. Yamamoto, K. Inomata, M. Watanabe, K. Matsuba, T. Miyazaki, W. D. Oliver, Y. Nakamura, and J. S. Tsai, *Appl. Phys. Lett.* **93**, 042510 (2008).
- ⁹N. Bergeal, F. Schackert, M. Metcalfe, R. Vijay, V. E. Manucharyan, L. Frunzio, D. E. Prober, R. J. Schoelkopf, S. M. Girvin, and M. H. Devoret, *Nature* **465**, 64–68 (2010).
- ¹⁰M. A. Castellanos-Beltrana and K. W. Lehnert, *Appl. Phys. Lett.* **91**, 083509 (2007).
- ¹¹L. Spietz, K. Irwin, and J. Aumentado, *Appl. Phys. Lett.* **93**, 082506 (2008).
- ¹²L. Spietz, K. W. Lehnert, I. Siddiqi, and R. J. Schoelkopf, *Science* **300**, 1929–1932 (2003).
- ¹³A. H. Steinbach, J. M. Martinis, and M. H. Devoret, *Phys. Rev. Lett.* **76**, 3806–3809 (1996).
- ¹⁴K. E. Nagaev, *Phys. Rev. B* **52**, 4740–4743 (1995).
- ¹⁵P. J. Burke, R. J. Schoelkopf, D. E. Prober, A. Skalare, B. S. Karasik, M. C. Gaidis, W. R. McGrath, B. Bumble, and H. G. LeDuc, *J. Appl. Phys.* **85**, 1644–1653 (1999).
- ¹⁶J. Teufel, Ph.D. dissertation, Yale University, 2008.
- ¹⁷R. Schoelkopf, P. Burke, A. Kozhevnikov, D. Prober, and M. Rooks, *Phys. Rev. Lett.* **78**, 3370–3373 (1997).
- ¹⁸N. Bergeal, R. Vijay, V. E. Manucharyan, I. Siddiqi, R. J. Schoelkopf, S. M. Girvin, and M. H. Devoret, *Nat. Phys.* **6**, 296302 (2010).
- ¹⁹B. Abdo, F. Schackert, M. Hatridge, C. Rigetti, and M. H. Devoret, *Appl. Phys. Lett.* **99**, 162506 (2011).
- ²⁰H. Pothier, S. Gueron, N. O. Birge, D. Esteve, and M. H. Devoret, *Phys. Rev. Lett.* **79**, 3490–3493 (1997).